NONPROTON ION RELEASE BY PURPLE MEMBRANES EXHIBITS COOPERATIVITY AS SHOWN BY DETERMINATION OF THE OPTICAL CROSS-SECTION

TIM MARINETTI
The Rockefeller University, New York 10021

ABSTRACT The amplitudes of the conductivity transients in photoexcited purple membranes were studied as a function of the energy of the actinic flash to determine the optical cross section of the process giving rise to the conductivity transient. Heating of the solution by the absorbed light causes an additional conductivity change and serves as an internal actinometer; the experiment directly yields the ratio of the cross section of ion release/uptake to that for light absorption. In effect, this counts the number of bacteriorhodopsin (bR) molecules involved in the conductivity transient per photon absorbed. At pH 7 in 0.4–0.5 M NaCl, where the conductivity signals are dominated by nonproton ions, the ratio is between 3 and 4, i.e., excitation of any one of several chromophores generates the same ion release signal. The simplest interpretation is that at pH 7 cooperative conformational changes cause a transient change in the surface charge distribution near all the affected bR molecules, resulting in the transient release of numerous counterions. As a comparison, at pH 4 where the signals are due to protons alone, the cross section data indicate that only a single bR molecule is involved in the proton movements. In this case, the results also show that the sum of the primary forward and reverse quantum yields (for the reactions: bR $\leftrightarrow$ K) is 0.88 $\pm$ 0.09.

INTRODUCTION

Bacteriorhodopsin (bR) is the light-driven proton pump and the sole polypeptide component of the purple membrane (PM) in *Halobacterium halobium* (1). In native PM, the bR molecules are arranged in trimers, which form a hexagonal two dimensional crystal lattice (2). Each bR contains a retinal molecule covalently coupled to the protein via a Schiff base with a lysine residue. Neighboring chromophores in a trimer interact, as indicated by the circular dichroism band at 600 nm (3, 4).

The trimeric structure of the PM is not an absolute requirement for proton pumping since bR monomers in lipid vesicles translocate H^+ (5). Nonproton ions also move on and off the protein during the photocycle. This was suggested by Slifkin et al. (6, 7) from light modulation conductivity experiments and subsequently proven in our laboratory by direct observation of the conductivity transients after an actinic flash (8–10). Above pH 7 or at ionic strengths above 0.2 M, the nonproton ion signal corresponds to release followed by uptake with quantum yields far in excess of 1 (8–10). This large nonproton ion release is abolished when bR is solubilized in detergent (9) or reconstituted as monomers in phospholipid vesicles (11), and thus appears to be associated with the aggregated structure of the PM.

Earlier we postulated that the nonproton signals were due to conformationally driven changes in the surface charge distribution in the PM during the photocycle which cause concomitant changes in the population of counterions trapped near the membrane surface (9). Observation of quantum yields as high as 10 ions per photon absorbed (9) would be difficult to explain on the basis of one bR molecule since the total charge transiently released approaches the total net charge of the protein. That is, one would have to postulate that nearly the entire net charge on one bR molecule's surface would have to be transiently neutralized during the photocycle, allowing transient release of the counterions. However, if the conformational changes causing the nonproton ion release also occur in other bR molecules neighboring the one excited by light, it could explain the high ion yields since the observed signals would be the sum of the responses from several bR molecules. Ahl and Cone (12) observed linear dichroism changes which implied that excitation of one chromophore induced rotations not only in itself but also in its neighbors. This supports the possibility of cooperativity in light-induced conformational changes during the photocycle.

Here, direct experimental evidence is presented indicating that more than one bR molecule is involved in the nonproton ion release. The optical cross section for the nonproton ion signal at pH 7 is 3 to 4 times as large as that for the production of heat from degradation of the absorbed light. The cross section for heating is the same as the absorption cross section of a single bR molecule. At pH 4, where the signal is known to be solely due to protons (8), the cross sections for proton uptake and for thermal heating are similar. Hence at pH 4, the H^+ movements

involve only a single bR molecule. The simplest interpretation for the cross section of the nonproton ion movements is that excitation of one bR stimulates in two or more neighboring molecules the conformational changes which transiently alter the surface charge distribution of all affected bR molecules. The resulting transient release of counterions generates the observed conductivity signals.

MATERIALS AND METHODS

The conductivity apparatus, calculations, and bacteriorhodopsin preparation have been described previously (9, 10). In addition to the Phase-R 1200 VXH dye laser (Phase-R Corp., Durham, NH) normally used for the conductivity experiments, a Candela SLL-250 dye laser (Candela Corp., Natick, MA) was used to obtain higher energy flashes. Both lasers used Rhodamine 590 dye (Exciton Chemical Co., Dayton, OH), lasing nominally at 590 nm. The flashes were attenuated with culture flasks containing metal sulfate salt solutions (30 mM $CrSO_4$, 22 mM $NiSO_4$, 13 mM $CoSO_4$, and 8 mM $CuSO_4$ in 10 mM H_2SO_4 and dilutions thereof [A. C. Ley, personal communication]). All experiments were performed at 16.0° or 17.0°C. Calculations were performed on Osborne 1 and IBM PC-AT computers.

RESULTS AND DISCUSSION

The conductivity of a solution is proportional to the sum of the concentration of each ion times a factor related to its mobility. The actinic flash induces changes in both terms of the product: (*a*) concentration changes due to ions transiently released from the PM surface and, (*b*) mobility changes due to the minute heating of the solution due to the light energy absorbed by the bR molecules. The former appears as a time-resolved transient; the latter as a shift in the baseline during and after the flash. For a given flash energy, and hence temperature rise, the thermal step will scale with the bulk conductivity (which is measured for each sample). The thermal baseline shift thus can be used to determine the total number of photons absorbed in the sample. In practice, the thermal step is measured long after the photocycle is over when all intermediates have decayed back to bR, so the entire energy of the absorbed photons has been converted to heat (8). Hence, the conductivity method has an internal actinometer; no absolute measurement of light energy is necessary.

By measuring the amplitude of the transient signal as a function of light energy, the optical cross section can be determined. In essence, one measures the effective "target size" for the particular observable quantity. At low light intensity, the response will be linear; at very high intensity it must saturate since every target is hit and increasing the number of photons can give no more additional response. The analysis of this problem, with application to photosynthetic systems, has been given in detail by Mauzerall (13, 14) using Poisson statistics and will be used here.

In our experiments, the flash duration is 0.5 μs and even at the highest light intensities available, each bR receives on average <10 hits per flash, i.e., 50 ns between successive hits. Since the excited state in bR decays to spectroscopically distinct intermediates in a few picoseconds (15), multiple hits during the excited state lifetime can clearly be neglected. The operational parameter is then the product of the optical cross section (σ) times the total number of photons per unit area (E), i.e., the integral of the flash intensity over time. After Mauzerall (13, 14), the product σE is denoted x, which by definition is the average number of hits per target. The probability that a target is hit n times is given by the Poisson factor $P_n = x^n \exp(-x)/n!$. Note that the cross section is the target size for the particular observable process and is not necessarily equal to the cross section for absorption of a single chromophore. For example, in photosynthetic systems, the measured cross section for oxygen evolution is the cross section per trap (13) and involves several hundred chlorophyll molecules (16).

For the simple case where one or more hits gives the same effect and for optically thin samples, the yield vs. flash energy is the cumulative one hit Poisson sum (13), i.e., $1 - P_0$, the latter term being the fraction of targets not hit at all, multiplied by an amplitude scale factor:

$$Y = Y_0[1 - \exp(-b\sigma E)], \quad (1)$$

where Y_0 is the amplitude of the signal at saturation, and the optical cross section has been explicitly separated into the true absorption cross section σ times a factor b. For the case of no photoreversal, the b factor is equal to the forward quantum yield of the primary photoreaction which eventually leads to the observed signals.

The effect of a 0.5 μs flash on light-adapted bR (bR^L) will be more complicated because the photocycle intermediates are interconvertible by light. In addition, they will have different cross sections at the actinic wavelength since their absorption spectra are different (15, 17–20). At the excitation wavelength (590 nm), however, all relevant species but one have almost the same extinction coefficient (15, 17, 18, 20); that of L is less by about a factor of 2. The simple case of Eq. 1 assumes that the cross section is constant and independent of the number of hits. Were there photocycle intermediates such as L or especially M present to any appreciable extent during the flash, then the light saturation would be complex, since the sample would tend to become invisible to the laser wavelength as the blue-shifted intermediates accumulated. All these effects would make the saturation curve (amplitude vs. flash energy) deviate below that expected from Eq. 1 since more light would be needed to drive the system into saturation. A derivation of the expected saturation behavior is given in the Appendix for a scheme involving all intermediates important on the microsecond timescale at room temperature.

The primary photochemistry of bR is currently in dispute, specifically over the question of the nature of the J intermediate (15, 20, 21) and of the forward quantum yield for bR $\rightarrow$ K. Several reports (18, 19, 22) claim that the forward quantum yield is 0.3 and that of the photoreversal of K to bR is ~0.7. Other workers (15, 23, 24) cite

evidence for the forward quantum yield being closer to 0.6. Since the cross sections measured in the experiments presented here depend on the forward and reverse quantum yields (see Appendix), an estimate can be made on the value of the sum of the two.

To calculate the average number of hits, we proceed as follows. Since the quantum yield of fluorescence for bR is very small ($<10^{-4}$) (15, 25), all photons absorbed are eventually degraded to heat. This causes a small temperature rise, which in turn increases the bulk conductivity (K) of the sample by a small amount (ΔK). Using the thermal coefficient of ionic mobility, $d \ln \Lambda / dT$ (which is 0.022 $°C^{-1}$ for all small ions except H^+ and OH^-), the average number of hits is:

$$x_T = (\sigma_T E) = (\Delta K/K)\, \rho\, C/[n\, \epsilon\, (d \ln \Lambda/dT)], \qquad (2)$$

where ρ is the density of the solution (gm/cm^3), C is the heat capacity per gram, n is the number of bR molecules per cm^3 and ϵ is the photon energy. With the bR concentration, B_0, in μM and $\Delta K/K$ in ppm, Eq. 2 reduces to:

$$x_T = 0.938\, (\Delta K/K)/B_0 \qquad (3)$$

Note that the cross section contained in x_T above is that for thermal heating, which is equal to the absorption cross section of a single bR molecule. The experimental procedure is to measure the transient signal amplitude while varying the flash energy, using the thermal step at each point to calculate x_T. The data are then fit to Eq. 1, with the saturation amplitude, Y_0, and the factor b as adjustable parameters.

Fig. 1 shows the results of experiments at pH 4, where the conductivity transients are known to be solely due to

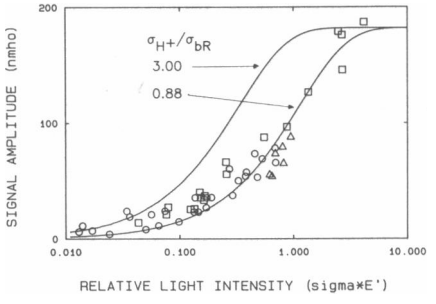

FIGURE 1 Light saturation of bR at pH 4. *Circles, triangles* (2 separate experiments): in 5 mM NaCl, 3.8 uM bR. *Squares:* in 10 mM NaCl, 5 μM bR. Signal amplitudes are calculated from nonlinear least squares fits to the conductivity transient and are scaled to 5 μM bR. The horizontal axis is the relative light intensity, σE, which equals the average number of photons absorbed per bR (see Eq. 2). Note that this is calculated directly from the conductivity data, not from external measurement of the actinic flash energy. The two curves are calculated using Eq. 1 with the optical cross section equal to 3 times (*left*) and 0.88 times (*right*) the thermal heating cross section, which is the absorption cross section for a single bR molecule. The right curve is the nonlinear least squares best fit to the data points. The saturation amplitude for both curves is 182.1 nmho. Each point represents the average of typically 64 flashes, except for the points at the lowest and highest flash energies, for which the number was greater or lesser, respectively, by multiples of 2.

H^+ (8). Optical spectra of light-adapted samples showed a maximum at ~570 nm and the ratio of absorbance at 605 nm to that at 568 nm was very similar to the ratio for the samples at pH 7 described below. This indicates that the amount of the blue acid form of bR which absorbs maximally at 605 nm (26) is negligible in the pH 4 samples. Fig. 1 includes data at 10 mM NaCl (*squares*) and 5 mM (*circles and triangles*), the latter measured on two different days to check reproducibility. The solid curves are calculated using the nonlinear least squares best fit b value of 0.88 ± 0.09, and also for $b = 3$. Note that in this experiment, the highest flash energy was sufficient to generate an average of four hits per bR, which should be within 98% of saturation for a simple cumulative one hit Poisson distribution. Thus, the saturation amplitude is fairly well constrained by the data and this places strict limits on the values of b which can fit the data.

As shown in the Appendix, the observed cross section will be the product of two terms: the sum of the forward and reverse quantum yields of the primary photoreaction, and the true absorption cross section, i.e., $\sigma_{obs} = (\phi_{12} + \phi_A)\, \sigma_1$. If N bR molecules act cooperatively in generating the conductivity transients, then σ_1 will be $N\sigma_{bR}$. Hence the b value from the fit to Eq. 1 is simply $(\phi_{12} + \phi_A)\, N$, which for Fig. 1 was 0.88. If N was 3, for example, it would mean that the sum of the quantum yields would have to be 0.29. This is too low; the forward yield, ϕ_{12}, is between 0.3 and 0.6 by itself, and the reverse yield is if anything larger than the forward yield (19). The same arguments rule out $N = 2$. The best explanation of the observed b value is that for H^+ uptake at pH 4, N is 1 and the sum of the primary quantum yields is 0.88.

One potential complication in this experiment is the presence of dark-adapted bR (bR^D), particularly when the succession of actinic pulses used in signal averaging is delivered at low energy. Dark adaptation during the flash sequence can be ignored since even at pH 4, where dark adaptation is faster, that time (100 s; [27]) is much greater than the pulse spacing (5 s). At moderate to high flash energies, the actinic light is sufficient to drive all bR to bR^L after a few flashes. (The first eight flashes are routinely discarded for this reason.) The data at low flash energy can be used to check for the presence of significant amounts of bR^D by calculating the power law dependence of the signal amplitude on σE. For a simple scheme $bR^D \rightarrow bR^L \rightarrow K$ where all bR starts as bR^D, the signal amplitude (proportional to the population of K and subsequent intermediates) should be quadratic in σE in the limit of low energy, independent of the various primary quantum yields. This prediction was confirmed by numerical integration of the scheme in Eq. A-1 (including bR^D) as a function of energy for $\sigma E < 0.2$. Log-log plots of the calculated intermediate population vs. σE gave slopes 1.94 and 1.91 using values of the forward quantum yields of 0.3 and 0.6, respectively. In contrast, the data of Fig. 1 gave a best fit slope of 0.6 ± 0.1; by eye the slope had to be 1 or less. Even with the

considerable scatter in the data, due to the low signal to noise ratio at $\sigma E < 0.2$, the observed data conclusively rule out a quadratic power law. These considerations argue against the presence of any appreciable amount of bR^D in these experiments.

The yield of ions per hit is obtained by fitting the ratio of the transient amplitude to the thermal step using the following function of the average number of hits:

$$R = R_0 [1 - \exp(-bx_T)]/(bx_T) \quad (4)$$

This is simply Eq. 1 divided by the average number of hits (see reference 13). The limiting ratio at zero flash energy, R_0, is directly related to the quantum yield of the ion transiently released (8):

$$\phi\Lambda_E = R_0 N_0 \epsilon/(1{,}000\, C\, \rho) \sum_i c_i\Lambda_i (d \ln \Lambda_i/dT), \quad (5)$$

where N_0 is Avogadro's number, c_i and Λ_i are the concentration and equivalent conductance of ion i, ϕ and Λ_E are the quantum yield and effective equivalent conductance of the ion transiently released (see reference 9) and the other terms are defined above. It is important to note that the quantum yield referred to in Eq. 5 is a product yield for ion release/uptake. These events occur in time beyond the K intermediate. The quantum yields referred to previously (ϕ_{12} and ϕ_A) are different: they have to do with photoconversions between bR^L and the early intermediates of the photocycle.

Due to the low ionic strength of the samples of Fig. 1, the thermal baseline shift was very small, particularly at low flash energy, and use of Eq. 4 was precluded by the large scatter in the data. A rough lower bound on the quantum yield of H^+ uptake is 0.13 or more. This was calculated by averaging the observed ratios in the range $x_T = 0.05$ to 0.3, where the ratios should be close to the limiting value. The major uncertainty is that the effective equivalent conductance for a proton is not known since this sample contained no external buffers. The above yield assumes the mobility of a free proton; the presence of trace buffer species would lower the effective equivalent conductance of protons since buffer ions have smaller mobilities than H^+. This would increase the calculated quantum yield. The previous measurement of the quantum yield for protons at pH 4 in acetate buffer was 0.4 (8).

Fig. 2 shows the results for bR in 0.5 M NaCl at pH 7 (two samples). Under these conditions, the transient signal is known to be dominated by the large nonproton ion release (9, 10). Here the best fit for b was 3.17 ± 0.38. (The two data sets gave b values of 3.16 and 3.22 when fit separately). The solid curve to the right is calculated using $b = 1$ for comparison. For these samples, the highest x_T value attained was 1.5 which is only 77% of saturation for $b = 1$. Also, there is scatter in the signal amplitudes. Hence the saturation amplitude is not as well constrained as in Fig. 1 and this could influence the best fit b value.

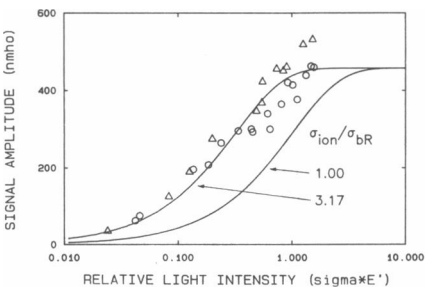

FIGURE 2 Light saturation of bR in 2.3 mM imidazole, 0.5 M NaCl, pH 7. *Circles:* 12.7 μM bR; *triangles:* 19.7 μM bR. Signal amplitudes are scaled to the higher bR concentration. Solid curves calculated from Eq. 1 using optical cross sections 3.17 times (*left*) and 1.0 times (*right*) the thermal cross section. The left curve is the best fit to the points. The saturation amplitude for both curves is 457.3 nmho.

However, it is very clear that the data are very far from the $b = 1$ curve.

Because the samples of Fig. 2 are at high ionic strength, the thermal amplitudes are well determined at all flash energies and Eq. 4 can be reliably used to fit the data. This has the advantage that the fit is insensitive to the saturation amplitude: the function is constrained by the limiting ratios at low flash energy. The results are shown in Fig. 3 and the curves are calculated for the best fit $b = 4.22 \pm 0.24$ and $b = 1$. Error bars on the data points are shown only when the error was larger than the symbol itself. Despite the lower signal to noise ratio at low flash energy, the limiting ratio is quite well determined. To fit the data with $b = 1$, the limiting ratio would have to be well below the observed data points. The difference in the b value between the fits to Figs. 2 and 3 can be attributed to the fact that this parameter is most sensitive to the high energy portion of the data in Fig. 2, but the low energy region in Fig. 3.

The main point is that in both cases, using two different forms of the light saturation function, the observed b value ($=[\phi_{12} + \phi_A]N$) is between 3 and 4. If the primary quantum yields are similar at pH 4 and 7, these factors will

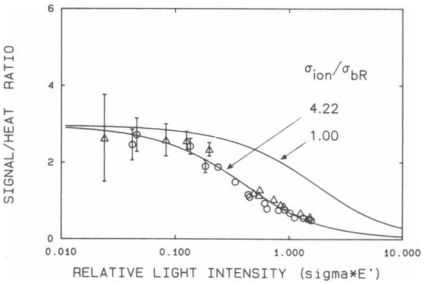

FIGURE 3 Light saturation of ion yield per hit. Ratio of transient amplitude to thermal baseline shift, directly related to quantum yield. Data from Fig. 2, replotted using Eq. 4. Error bars indicated except where error less than symbol size. The solid curves are calculated for optical cross sections 4.22 times (*left;* best fit) and 1.0 times (*right*) the thermal cross section. The limiting ratio at low flash energy is 2.97 for both curves.

cancel out in the ratio of the observed cross section of ion release (Fig. 2) to that for H^+ uptake (Fig. 1). This ratio directly measures the ratio of the number of bR molecules involved in the two processes. Since there must be at least one bR involved in the proton uptake, this gives an absolute requirement that the number of bR molecules involved in the ion release transient must be 3 to 4. Within the limitation that the sum $\phi_{12} + \phi_A$ is not very different at the two pHs, this conclusion is insensitive to the individual values of the quantum yields ϕ_{12} and ϕ_A. Thus, the conclusion is independent of the details of the composition of the photostationary state formed during the actinic flash. Using the standard deviations of the fits as the errors, the number of bR molecules involved in the nonproton ion release is 3.7 ± 0.6. Note that regardless whether the sum of quantum yields is different at pH 4 than pH 7, the maximum value of $\phi_{12} + \phi_A$ is 2, so the absolute minimum number of bR molecules involved in the pH 7 signals is 1.5 to 2.

Fig. 4 shows the results of similar experiments with bR in 0.4 M NaCl at pH 7. As in Fig. 3, the ratio of the transient amplitude to the thermal step is plotted. The curves are calculated using b values of (*left to right*): 5, 4.09 (best fit), 3 and 1. Due to the lower bR concentration, the signal to noise ratio was lower, as seen in the scatter at low flash energy and in the higher error of the fit b (±0.53). The curves calculated for $b = 5$ and 3 show clearly that the actual value is bracketed within this range.

The limiting signal to heat ratios from Figs. 3 and 4 are 2.97 and 3.43, respectively. Assuming that the transient is due entirely to counterion release, these ratios correspond to quantum yields of 3.5 and 3.9 ions per photon absorbed. This is about half the yield observed at the same pH in 1 M NaCl (9).

The error limits noted above are purely the statistical errors generated by scatter in the data. The major source of systematic error in determination of optical cross sections is normally the difficulty of ascertaining the number of photons actually absorbed by the sample. Thus, a great advantage of the method used here is that no measurement of the absolute flash energy, corrections for reflections at optical surfaces, etc. are required. The thermal heating directly observed in these experiments is determined only by the absorbed light. In the signal to heat ratios of Figs. 3 and 4, all geometrical factors, effects of inhomogeneous illumination and the like explicitly cancel out. The major sources of systematic error are eliminated by virtue of determining the optical cross section relative to that of thermal heating.

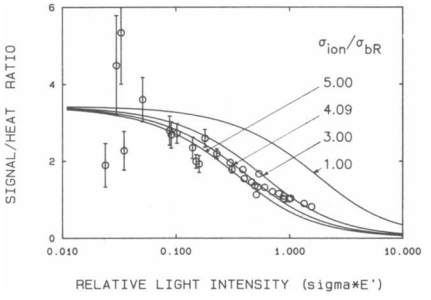

FIGURE 4 Light saturation of ion yield per hit. bR (10 μM) in 2 mM imidazole, 8.9 mM Na phosphate, 19 mM glycinamide, 0.4 M NaCl, pH 7. Data are plotted according to Eq. 4 as in Fig. 3. From left to right, the solid curves are calculated using cross sections 5, 4.09, 3 and 1.0 times the thermal cross section. The best fit to the data is for $b = 4.09$. The limiting ratio for all curves is 3.43.

Secondly, the points of Figs. 1 and 2 clearly correspond to cross sections which differ by a multiplicative factor, i.e., they are shifted relative to one another on the logarithmic horizontal axis. Systematic errors might shift the absolute value of the cross section, but since these errors should affect the experiments of Figs. 1 and 2 in the same way, the relative horizontal displacement of the two data sets would still be preserved.

All of the above calculations have assumed that the optical cross section is isotropic. However, on the 0.5 μs timescale the PM fragments are essentially immobile and this could result in complications from photoselection. This problem has been analyzed by Nagle et al. (28), and using their equations, the light saturation curve was calculated by numerical integration. The worst case deviation from isotropic behavior for unpolarized flashes is only 10% near the upper part of the saturation curve, and this assumes the actinic light is perfectly collimated. In reality, the actinic pulse undergoes reflections off the brass walls of the thermostat and is scattered by the bR itself, all of which tends to homogenize the light. For this reason, deviations due to photoselection have been ignored. In addition, since our data are plotted versus the experimentally measured average number of hits, not the flash energy alone, any effects of photoselection are automatically taken into account.

The data presented above indicate that the sum of primary quantum yields is 0.88 ± 0.09 at pH 4. This can be compared with other reported quantum yield data, assuming that these parameters do not change greatly between pH 4 and pH 7. The ratio of the forward to the reverse quantum yield is 0.4 at room temperature, as reported by Goldschmidt et al. (18). Even if the forward yield is simply assumed to be less than the reverse, the result of this experiment is that the forward yield would have to be <0.44. Birge and Cooper (29) determined the sum of the quantum yields to be 1.02 ± 0.19 at 77°*K* using photocalorimetry. Subsequent global optimization of their data (30) showed that the ratio of the forward to reverse quantum yield is 0.445 ± 0.031. Using this ratio, and the sum observed here, one calculates that the forward quantum yield, ϕ_{12}, is 0.27 ± 0.03. This is clearly more consistent with the values near 0.3 (19, 22) than those of 0.6 or more (23, 24). Assuming that the room temperature data and 77°*K* data are comparable, this calculated value of ϕ_{12}

would correspond to an enthalpy difference of 17 to 20 kcal/mol between bR and K (see e.g., Table III of reference 29).

The clear conclusion from these experiments is that the optical cross section for the nonproton ion release is larger than that of a single bR molecule by a factor between 3 and 4, i.e., excitation of any one or all of these chromophores gives the same observable response. (At present, the signal to noise ratio limitations of our apparatus do not permit the light saturation of the small proton component of the signal to be examined at pH 7 in 0.5 M NaCl.) The most straightforward interpretation is that several bR molecules function as a unit in generating the surface charge changes which lead to transient nonproton ion release. It is tempting to infer that the bR trimers are the functional unit, but the cross section data itself obviously cannot distinguish between bR molecules within one trimer from those in adjacent trimers. The possibility that several bR molecules might be involved in the nonproton ion release fits very well with the idea that the cause of the signal is a conformationally driven change in the surface charge distribution: the larger the affected area, the larger the number of counterions released and bound. This question and the evidence for conformational changes during the photocycle has been discussed previously (10).

Apparent cooperative interactions between nearby bR molecules in the PM have been reported, starting with the exciton interaction between chromophores in the trimers (3, 4). Subsequently, Rehorek and Heyn (31) showed that regeneration of bR by addition of retinal to the apo-protein is highly cooperative, with a Hill coefficient of 3. Evidence also exists of cooperative interactions during the photocycle, e.g., the dependence of M decay kinetics on the fraction of the bR present as M in the photostationary state (32) and the experiments of Ahl and Cone (12) noted above. The experiments presented here demonstrate functional cooperativity involving excited bR molecules and neighbors in the generation of transient ion movements. To our knowledge, this is the first direct proof of cooperative interactions involving the chromophore and events at the surface of the PM in actively cycling conditions.

APPENDIX

Light Energy Dependence of the Population of bR Photocycle Intermediates After a Flash

The effect of illumination of a light-adapted bR (bR^L) sample is to initiate a cycle of spectroscopically distinct intermediates which exist on timescales from picoseconds to milliseconds. Besides the light-independent (dark) reactions, in which intermediates decay into each other, during the flash conversions can take place wherein one intermediate absorbs a photon and is converted into another intermediate or back to bR^L. Only those bR molecules present after the flash as one of the various intermediates will go on to complete the photocycle. These in turn are the only source of the observable transient conductivity changes. Hence, we need to calculate the total fraction of bR which exists as one or another of the intermediates after the flash as a function of the actinic flash energy E.

On the 0.5 μs timescale of our laser flash, only the following intermediates will be relevant at room temperature:

$$bR^L \xrightarrow[0.7\ ps]{} J \xrightarrow[5\ ps]{} K \xrightarrow[<150\ ns]{} K' \xrightarrow[2.2\ \mu s]{} L \qquad \text{(A-1)}$$

Note that K' is the KL intermediate observed by Shichida et al. (20) which is spectroscopically similar to the classical K precursor to L (17). The precursor to K' decays in <150 ns and has been included since it might live long enough to undergo photoreversal to bR^L. If there were no photoreversal, the observed light energy dependence of the signal amplitude would show a simple Poisson saturation (Eq. 1) with a cross section given by the absorption cross section multiplied times the forward quantum yield (c.f., Mauzerall [14]).

The nature of J is the subject of current debate in the literature. Polland et al. (15) cite it as the first ground state intermediate, whereas Birge et al. (21) argue that it is a metastable form of the excited singlet state. For the experiments here, the distinction is moot: J decays is 5 ps and hence does not live long enough to undergo photoreversal even at the highest light energies used here, wherein the bR molecules are hit once every 50 ns on average. Whether J is an intermediate directly on the pathway to K, or if it is an alternate pathway for relaxation of the excited singlet back to bR^L, will of course affect the yield of later intermediates. For our purposes, this can be taken into account by using as effective forward quantum yield ϕ_{12} for the formation of K from bR^L.

The flash is assumed to be a square pulse of total energy E (in photons per unit area) $= \int_0^T I(t)\,dt$ where T is the flash length. If we divide the flash into short intervals dt, the number of photons illuminating the targets in the interval is simply $E(dt/T)$. The number of hits received by species i is Poisson distributed and the loss in concentration of species i to species j caused by photoconversion during the interval dt is:

$$\Delta c_j(t) = c_i(t)\,\phi_{i,j}[1 - \exp(\sigma_i E\,dt/T)], \qquad \text{(A-2)}$$

where $\phi_{i,j}$ is the quantum yield for conversion of i to j and σ_i is the absorption cross section of i. In addition to the light driven changes, the first order dark decay of i to j will give a loss term:

$$\Delta c_j(t) = k_{ij}\,c_i(t)\,dt \qquad \text{(A-3)}$$

For the bR photocycle, the first order rate constant k_{ij} will generally be 0 unless $j = i + 1$. The total change in $c_i(t)$ is

obtained by summing the losses and gains from all possible light-driven and dark decay processes which couple species i to other intermediates.

If the interval dt is made very short, the exponential terms in Eq. A-2 can be linearized. Taken to the limit $dt \rightarrow 0$, one obtains a set of coupled linear differential equations for the concentrations of each intermediate as a function of time. Neglecting J, the result for the population of bR^L is:

$$d bR^L/dt = [-bR^L(t)\,\phi_{12}\,\sigma_1 + \sum_{i=2}^{4} c_i(t)\,\phi_{i1}\,\sigma_i]\,E/T, \quad \text{(A-4)}$$

where 1 refers to bR^L, 2 to K, 3 to K', and 4 to L.

Noting that the total bR is conserved ($B_0 = bR^L + K + K' + L$) this equation can be recast into one for the rate of change of the sum of K, K', and L:

$$d(K + K' + L)/dt = [B_0\,\phi_{12}\,\sigma_1 - (K + K' + L)\,\phi_A\,\sigma_A]E/T + f(t), \quad \text{(A-5)}$$

where $\phi_A\,\sigma_A = g_2\phi_{21}\sigma_2 + g_3\phi_{31}\sigma_3 + g_4\phi_{41}\sigma_4$, and $f(t)$ is an error term:

$$f(t) = \left(\frac{1}{2}\right)(E/T)\sum_{i=2}^{4}\sum_{j=2}^{4} \cdot (\phi_{j1}\sigma_j - \phi_{i1}\sigma_i)[g_j\,c_i(t) - g_i\,c_j(t)]. \quad \text{(A-6)}$$

Here, the g_i are weighting factors (between 0 and 1) which we will set proportional to the steady state populations of species i present at high light flash energy. To the extent that the error term is small, Eq. A-5 is a simple first order differential equation which can be readily integrated to give the total $K + K' + L$ present at the end of the flash, i.e., at $t = T$:

$$K(T) + K'(T) + L(T) = B_0\left(\frac{\phi_{12}\sigma_1}{\phi_{12}\sigma_1 + \phi_A\sigma_A}\right)\{1 - \exp[(-\phi_{12}\sigma_1 - \phi_A\sigma_A)E]\}. \quad \text{(A-7)}$$

This is a simple Poisson saturation curve with a cross section involving the absorption cross sections of bR^L, K, K', and L as well as the quantum yields for the forward and reverse reactions.

To a good approximation, the population of L can be ignored. Its formation time is ~2 μs at room temperature (20, 33, 34) so even if all bR molecules were converted to K at time zero, only 16% of the total would be present as L at the end of the 0.5 μs flash. However, the actual population of L will be considerably less since the forward quantum yield is <1 and the precursors of L are not formed at $t = 0$ but continuously throughout the flash. Furthermore, at the actinic wavelength used (590 nm), the absorption cross section of L is about half that of bR (15, 17, 21) which reduces the importance of possible photoreversal from L to bR^L.

The error term $f(t)$ is expected to be small on the following general grounds. At high light flash energies, the concentrations of each species will approach their steady state values and will be proportional to the weighting factors g_i. Therefore, each difference term in the summation in Eq. A-6 will tend to 0 regardless of the multiplicative factor involving the quantum yields and absorption cross sections. At low light energy, the population of all intermediates is small, and the error term which depends on their differences will likewise be small. As a test, the exact differential equations were integrated numerically including all species except J and allowing K a lifetime of the maximal value of 150 ns. The resulting populations of intermediates present at the end of the flash ($t = T$) were calculated as a function of the flash energy E and fit to a simple cumulative Poisson saturation (Eq. 1). In all cases, including a range of assumed values of the assorted quantum yields for the forward and reverse photoreactions, the numerically synthesized sum of K, K', and L fit the functional form of Eq. A-7 to within a few percent, which is less than the experimental error of the data reported here.

Note that if K and K' are essentially identical in terms of photoreversal, i.e., if $\phi_{21}\,\sigma_2 = \phi_{31}\,\sigma_3$, then the error term $f(t)$ will be equal to 0. In this case, the saturation curve has the same form as Eq. 1 of Mauzerall (14), which was derived for photoreversal involving two species using a kinetic scheme. Mauzerall's rate constants σI are equal to the terms $\phi\sigma E/T$ in our notation since he included the quantum yields in his cross sections, whereas here, the cross sections are the true absorption cross sections to which the quantum yields have to be added as multiplicative factors.

At the actinic wavelength used (590 nm) the reported extinction coefficients for bR^L, K, K', and J are all very similar (16, 21). Hence σ_1, σ_2, and σ_3 can be taken as approximately equal. Neglecting J and L, $g_4 = 0$ in the sum defining $\phi_A\sigma_A$. Taking $g_2 = 1 - g_3 = \phi_{31}/(\phi_{21} + \phi_{31})$, the cross sections then factor out of the composite term for K and K' and ϕ_A is then equal to the self-weighted average of ϕ_{21} and ϕ_{31}:

$$\phi_A = 2\,\phi_{31}\,\phi_{21}/(\phi_{31} + \phi_{21}). \quad \text{(A-8)}$$

From Eq. A-7, this means that the observed cross section for the conductivity transients will simply be $\sigma_1\,(\phi_{12} + \phi_A)$. For a process which involves bR molecules as individuals, $\sigma_1 = \sigma_{bR}$, and the b value obtained from the fits to the data is a direct measure of $\phi_{12} + \phi_A$. In the numerical calculations referred to above, using values of the various quantum yields between 0.3 and 1, the fits to the synthesized populations of $K' + K + L$ gave b values within 2% of that expected from $\phi_{12} + \phi_A$ using Eq. A-8 to calculate the latter.

The ratios of signal amplitudes at different flash energies may be used to estimate the sum of quantum yields. At low flash energy, the signal amplitude (proportional to $K + K' + L$) depends only on ϕ_{12} as can be seen by linearizing the exponential term in Eq. A-7. However in

the saturation region ($\sigma_1 E > 1$), the ratios will depend on how much the sum of quantum yields differs from 1. For the experiment in Fig. 1 where the data extends to $\sigma E = 4$, the ratio of the observed amplitude at $\sigma E = 4.2$ to that at $sE = 1$ is 1.8 ± 0.1. From this, one estimates that $\phi_{12} + \phi_A$ is between 0.74 and 0.9, which is consistent with the best fit b value of 0.88.

I would like to acknowledge the technical help of Irene Zielinski-Large who grew the *H. halobium* and prepared the PM. Dr. David Mauzerall contributed his knowledge on optical cross sections and Poisson distributions. I also wish to acknowledge helpful comments from referees.

This work was supported by National Institutes of Health grant GM32955-03.

Received for publication 19 October 1987 and in final form 22 March 1988.

REFERENCES

1. Oesterhelt, D., and W. Stoeckenius. 1973. Functions of a new photoreceptor membrane. *Proc. Natl. Acad. Sci. USA.* 70:2853–2857.
2. Henderson, R. 1977. The purple membrane from *Halobacterium halobium. Rev. Biophys. Bioeng.* 6:87–109.
3. Heyn, M. P., P.-J. Bauer, and N. A. Dencher. 1975. A natural CD label to probe the structure of the purple membrane from *Halobacterium halobium* by means of exciton coupling effects. *Biochem. Biophys. Res. Commun.* 67:897–903.
4. Becher, B., and T. G. Ebrey. 1976. Evidence for chromophore-chromophore (exciton) interaction in the purple membrane of *Halobacterium halobium. Biochem. Biophys. Res. Commun.* 69:1–6.
5. Dencher, N. A., and M. P. Heyn. 1979. Bacteriorhodopsin monomers pump protons. *FEBS (Fed. Eur. Biochem. Soc.) Lett.* 108:307–310.
6. Slifkin, M. A., H. Garty, and S. R. Caplan. 1978. Modulation-excitation methods in the study of bacteriorhodopsin. *In* Energetics and Structure of Halophilic Microorganisms. S. R. Caplan and M. Ginzburg, editors. Elsevier/North-Holland Biomedical Press, Amsterdam. 165–184.
7. Slifkin, M. A., H. Garty, W. V. Sherman, M. F. P. Vincent, and S. R. Caplan. 1979. Light-induced conductivity changes in purple membrane suspensions. *Biophys. Struct. Mech.* 5:313–320.
8. Marinetti, T., and D. Mauzerall. 1983. Absolute quantum yields and proof of proton and nonproton transient release and uptake in photoexcited bacteriorhodopsin. *Proc. Natl. Acad. Sci. USA.* 80:178–180.
9. Marinetti, T., and D. Mauzerall. 1986. Large transient nonproton ion movements in purple membrane suspensions are abolished by solubilization in Triton X-100. *Biophys. J.* 50:405–415.
10. Marinetti, T. 1987. Abrupt onset of large scale nonproton ion release in purple membranes caused by increasing pH or ionic strength. *Biophys. J.* 51:875–881.
11. Marinetti, T. 1987. Large scale nonproton ion release and bacteriorhodopsin's state of aggregation in lipid vesicles. I. Monomers. *Biophys. J.* 52:115–121.
12. Ahl, P. L., and R. A. Cone. 1984. Light activates rotations of bacteriorhodopsin in the purple membrane. *Biophys. J.* 45:1039–1049.
13. Mauzerall, D. 1982. Statistical theory of the effect of multiple excitation in photosynthetic systems. *In* Biological Events Probed by Ultrafast Laser Spectroscopy. R. R. Alfano, editor. Academic Press, Inc., New York. 215–235.
14. Mauzerall, D. 1979. Multiple excitations and reaction yields in photosynthetic systems. *Photochem. Photobiol.* 29:169–170.
15. Polland, H.-J., M. A. Franz, W. Zinth, W. Kaiser, E. Kolling, and D. Oesterhelt. 1986. Early picosecond events in the photocycle of bacteriorhodopsin. *Biophys. J.* 49:651–662.
16. Ley, A. C., and D. C. Mauzerall. 1982. Absolute absorption cross-sections for photosystem II and the minimum quantum requirement for photosynthesis in Chlorella vulgaris. *Biochim. Biophys. Acta.* 680:95–106.
17. Lozier, R. H., R. A. Bogomolni, and W. Stoeckenius. 1975. Bacteriorhodopsin: a light-driven proton pump in *Halobacterium halobium. Biophys. J.*15:955–962.
18. Goldschmidt, C. R., M. Ottolenghi, and R. Korenstein. 1976. On the primary quantum yields in the bacteriorhodopsin photocycle. *Biophys. J.* 16:839–843.
19. Hurley, J. B., and T. G. Ebrey. 1978. Energy transfer in the purple membrane of *Halobacterium halobium. Biophys. J.* 22:49–66.
20. Shichida, Y., S. Matsuka, Y. Hikada, and T. Yoshizawa. 1983. Absorption spectra of intermediates of bacteriorhodopsin measured by laser photolysis at room temperatures. *Biochim. Biophys. Acta.* 723:240–246.
21. Birge, R. R., L. A. Findsen, and B. M. Pierce. 1987. Molecular dynamics of the primary photochemical event in bacteriorhodopsin. Theoretical evidence for an excited singlet state assignment for the J intermediate. *J. Am. Chem. Soc.* 109:5041–5043.
22. Goldschmidt, C. R., O. Kalisky, T. Rosenfeld, and M. Ottolenghi. 1977. The quantum efficiency of the bacteriorhodopsin photocycle. *Biophys. J.* 17:179–183.
23. Oesterhelt, D., and B. Hess. 1973. Reversible photolysis of the purple complex in the purple membrane of *Halobacterium halobium. Eur. J. Biochem.* 37:316–326.
24. Oesterhelt, D., P. Hegemann, and J. Tittor. 1985. The photocycle of the chloride pump halorhodopsin. II: Quantum yields and a kinetic model. *EMBO (Eur. Mol. Biol. Org.) J.* 4:2351–2356.
25. Govindjee, R., B. Becher, and T. G. Ebrey. 1978. The fluorescence from the chromophore of the purple membrane protein. *Biophys. J.* 22:67–77.
26. Mowery, P. C., R. H. Lozier, Q. Chae, Y.-W. Tseng, M. Taylor, and W. Stoeckenius. 1979. Effect of acid pH on the absorption spectra and photoreactions of bacteriorhodopsin. *Biochemistry.* 18:4100–4107.
27. Ohno, K., Y. Takeuchi, and M. Yoshida. 1977. Effect of light-adaptation on the photoreaction of bacteriorhodopsin from *Halobacterium halobium. Biochim. Biophys. Acta.* 462:575–582.
28. Nagle, J. F., S. M. Bhattacharjee, L. A. Parodi, and R. H. Lozier. 1983. Effect of photoselection upon saturation and the dichroic ratio in flash experiments upon effectively immobilized systems. *Photochem. Photobiol.* 38:331–339.
29. Birge, R. R., and T. M. Cooper. 1983. Energy storage in the primary step of the photocycle of bacteriorhodopsin. *Biophys. J.* 42:61–69.
30. Birge, R. R., T. M. Cooper, C. M. Einterz, L. A. Findsen, M. B. Masthay, L. P. Murray, G. A. Schick, and C. F. Zhang. 1988. The nature of the primary photochemical events in rhodopsin and bacteriorhodopsin. *Biophys. J.* 53:1a. (Abstr.)
31. Rehorek, M. and M. P. Heyn. 1979. Binding of all-trans retinal to the purple membrane. Evidence for cooperativity and determination of the extinction coefficient. *Biochemistry.* 18:4977–4983.
32. Korenstein, R., B. Hess, and M. Markus. 1979. Cooperativity in the photocycle of purple membrane of *Halobacterium halobium* with a mechanism of free energy transduction. *FEBS (Fed. Eur. Biochem. Soc.) Lett.* 102:155–161.
33. Stoeckenius, W., and R. H. Lozier. 1974. Light energy conversion in *Halobacterium halobium. J. Supramol. Struct.* 2:769–774.
34. Xie, A. H., J. F. Nagle, and R. H. Lozier. 1987. Flash spectroscopy of purple membrane. *Biophys. J.* 51:627–635.